



Research Report

Thermodynamical Stability and Dehydrating Property of Calcium Borohydride $\text{Ca}(\text{BH}_4)_2$

Masakazu Aoki, Kazutoshi Miwa, Tatsuo Noritake, Hai-Wen Li and Shin-ichi Orimo

Report received on Dec. 10, 2013

■ABSTRACT■ We report our theoretical and experimental studies on the thermodynamical stability and dehydrating property of $\text{Ca}(\text{BH}_4)_2$. The polymorphic crystal structures of $\text{Ca}(\text{BH}_4)_2$ have been investigated by the synchrotron powder X-ray diffraction measurement. The crystal structures of α - $\text{Ca}(\text{BH}_4)_2$ and β - $\text{Ca}(\text{BH}_4)_2$ are refined at temperatures 300 and 433 K, respectively. The polymorphism of $\text{Ca}(\text{BH}_4)_2$ is formed by the different connection with adjacent octahedrons sharing vertexes and edges of the CaB_6 octahedron. Using the structural information, the first-principles calculations have been performed to investigate the fundamental properties of $\text{Ca}(\text{BH}_4)_2$. The dehydrating reaction is predicted to be $\text{Ca}(\text{BH}_4)_2 \rightarrow 2/3\text{CaH}_2 + 1/3\text{CaB}_6 + 10/3\text{H}_2$, which is supported by the thermogravimetric analysis and the pressure-composition (*p-c*) isotherm measurement. The CaH_2 phase and the orthorhombic intermediate phase appear in the XRD profile of the sample after the *p-c* isotherm measurement; this indicates that the partial dehydrogenation of $\text{Ca}(\text{BH}_4)_2$ accompanied by the formation of these two phases occurs during the *p-c* isotherm measurement.

■KEYWORDS■ Hydrogen Storage, Complex Hydride, Theoretical Calculations, Crystal Structure, Dehydrating Reaction

1. Introduction

Hydrogen is one of the clean and sustainable energy carriers in future to replace fossil fuels.⁽¹⁾ Hydrogen storage is essential technology for utilizing hydrogen. Especially, the development of safe and efficient hydrogen storage materials is indispensable for the popularization of fuel-cell vehicles. Up to now, various hydrogen storage materials have been investigated.⁽²⁾ Complex hydrides that consist of light elements have attracted considerable attention because of their high hydrogen density.⁽³⁾ Examples include alanates,⁽⁴⁻⁷⁾ amides⁽⁸⁻¹²⁾ and borohydrides.⁽¹³⁻²⁰⁾ Among borohydrides, alkali metal borohydrides such as LiBH_4 and NaBH_4 are well-known and their properties have been studied moderately. Although we can find borohydrides composed of not only alkali metals but also other types of metals in literature,^(21,22) little is known for the latter compounds. In this context, we have investigated the thermodynamical stability of several metal borohydrides, $\text{M}(\text{BH}_4)_n$ ($\text{M}=\text{Li}, \text{Na}, \text{K}, \text{Cu}, \text{Mg}, \text{Zn}, \text{Sc}, \text{Zr}$ and Hf), both theoretically and experimentally.⁽¹⁸⁾ It has been found that the stability of metal borohydrides shows a good correlation with the electronegativity of cation elements, *M*. From this correlation, it has been expected that calcium

borohydride $\text{Ca}(\text{BH}_4)_2$ is less stable than alkali metal borohydrides (LiBH_4 , NaBH_4 , KBH_4).

In this paper, we report our theoretical and experimental studies on the thermodynamical stability and dehydrating property of $\text{Ca}(\text{BH}_4)_2$.⁽²³⁻²⁵⁾ It is known that several polymorphisms such as α and β phases exist in $\text{Ca}(\text{BH}_4)_2$.⁽²⁶⁻²⁷⁾ For understanding of the thermodynamical stability and dehydrating property of $\text{Ca}(\text{BH}_4)_2$, it is important to clarify the structural change. Therefore, we present precisely analyzed crystal structures of α - $\text{Ca}(\text{BH}_4)_2$ and β - $\text{Ca}(\text{BH}_4)_2$ based on synchrotron X-ray diffraction (XRD) measurement.

2. Methods

2. 1 Experimental Procedure

The starting material of $\text{Ca}(\text{BH}_4)_2 \cdot 2\text{THF}$ was purchased from Sigma-Aldrich (product No. 389986). Adduct-free $\text{Ca}(\text{BH}_4)_2$ samples were prepared by heating the starting material under vacuum at 433 K for 10 h or at 523 K for 80 h. All the samples were handled in a glove-box filled with purified argon (dew point below 180 K).

The crystal structure and dehydrating properties of

$\text{Ca}(\text{BH}_4)_2$ were examined by XRD measurement (Rigaku RINT-TTR), the p - c isotherm measurement, thermogravimetry and differential thermal analysis (TG/DTA, Rigaku TG8120), and mass spectroscopy (MS, ANELVA M-200QA, directly connected with the TG/DTA apparatus). The XRD measurements were carried out with Cu $K\alpha$ radiation at room temperature. The volumetric method with a Sieverts apparatus (LESCA CORPORATION) was used to obtain the p - c isotherm when $\text{Ca}(\text{BH}_4)_2$ was dehydrided at 593 K. Before the measurement, the sample was kept under a hydrogen (purity 99.99999%) pressure of around 9.5 MPa at 593 K. TG/DTA and MS measurements were performed under a helium gas flow with a heating rate of 5 K/min and the equipment was installed inside the glove-box. The details of the p - c isotherm measurement, TG/DTA, and MS have been described in Refs. (28)-(30).

For more detail crystal structure analysis, the synchrotron X-ray diffraction experiment was carried out by use of a large Debye-Scherrer camera with an imaging plate as detectors at the beam-line BL02B2 and BL19B2 in SPring-8.⁽³¹⁾ The powder X-ray diffraction was measured at room temperature (300 K) and high temperature (433 K) with incident X-ray of wavelength 0.80Å. The temperature controlled nitrogen gas blower was used for high temperature measurement. The diffraction data were collected with a 0.01° step from 3.0° to 73.0° in 2θ .

From measurement data, the crystal structure of α - $\text{Ca}(\text{BH}_4)_2$ was analyzed by the Rietveld method using a computer program RIETAN.⁽³²⁾ The parameters related to background intensity were fixed in the Rietveld refinement. Because the sample was not single phase, the peak profile and structural parameters of major phase were varied but those parameters of minor phases were fixed or partially constrained.

2.2 Computational Method

The first-principles calculations have been performed using the ultrasoft pseudopotential method⁽³³⁾ based on density functional theory.^(34,35) The generalized gradient approximation⁽³⁶⁾ is adopted for the exchange-correlation energy. For Ca, the $3s$ and $3p$ semicore states are treated as valence. The cutoff energies used in this study are 15 and 120 hartrees for the pseudowave functions and the charge density, respectively. The k -point grids for the Brillouin zone

integration are generated so as to make the edge lengths of the grid elements as close to the target value of 0.08 bohr⁻¹ as possible. These computational conditions give good convergence for the total energy within 1 meV/atom. The linear response calculation based on density-functional perturbation theory is used to obtain the dielectric properties.^(37,38) The phonon eigenmodes are obtained by solving the eigenvalue problem for the dynamical matrix which is calculated by the force-constant method.⁽³⁹⁾

3. Results and Discussion

3.1 Crystal Structure of α - $\text{Ca}(\text{BH}_4)_2$

The crystal structure of calcium borohydride at ambient conditions, α - $\text{Ca}(\text{BH}_4)_2$, was firstly investigated by laboratory X-ray diffraction (XRD) measurement⁽²³⁾ and then refined by synchrotron XRD.⁽²⁵⁾ The Rietveld analysis pattern for synchrotron XRD measurement is given in **Fig. 1**. The main phase is α - $\text{Ca}(\text{BH}_4)_2$ with space group Fddd (No.70). A small amount of β - $\text{Ca}(\text{BH}_4)_2$ (0.7 mass%) and $\text{Ca}(\text{BH}_4)_2 \cdot \text{H}_2\text{O}$ (5.9 mass%) is also detected. The obtained structural parameters for α - $\text{Ca}(\text{BH}_4)_2$ are summarized in **Table 1**, which agree well with the

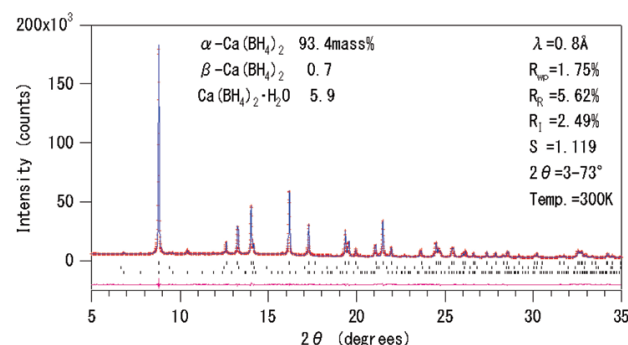


Fig. 1 Rietveld analysis pattern of the $\text{Ca}(\text{BH}_4)_2$ sample at 300 K.

Table 1 α - $\text{Ca}(\text{BH}_4)_2$ crystal data.

measurement temperature:	300K				
space group:	Fddd (No.70)				
lattice constant (Å):	a=8.7782(7)	b=13.129(1)	c=7.4887(6)		
atom	g	x	y	z	B[Å ²]
Ca	1.0	0.0	0.0	0.0	1.54(1)
B	1.0	0.0	0.2240(1)	0.0	2.30(3)
H1	1.0	-0.1115(5)	0.2690(3)	-0.0013(7)	2.4(1)
H2	1.0	-0.0025(7)	0.1736(3)	0.1241(7)	2.4

previous ones.⁽²³⁾ The crystal structure is shown in **Fig. 2**. A boron atom bonds with four hydrogen atoms and forms a BH_4 tetrahedron, where the B-H bond lengths and the H-B-H bond angles in BH_4 complexes are 1.14 Å and 106.9-109.1°, respectively. Six boron atoms around a calcium atom coordinate in octahedral type.

3.2 Theoretical Predictions for $\alpha\text{-Ca}(\text{BH}_4)_2$

The structural optimization is performed on $\alpha\text{-Ca}(\text{BH}_4)_2$ starting from the experimental geometry, where the atomic positions and the lattice vectors are fully relaxed. **Table 2** shows the calculated structural parameters, which are in fairly good agreement with the measured ones. The calculated B-H bond lengths and the H-B-H bond angles are 1.23-1.24 Å and 106-113°, respectively. The experimental B-H bond lengths are somewhat shorter than the predicted ones. This is probably caused by the experimental difficulty in identifying H positions due to their weak X-ray scattering power.

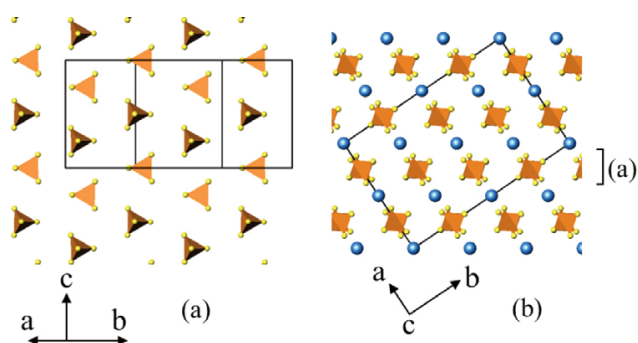


Fig. 2 (a) The arrangement of BH_4 tetrahedrons within the parallel plane to the (110) plane, (b) the stacking of planes in $\alpha\text{-Ca}(\text{BH}_4)_2$. The blue and yellow spheres represent Ca and H atoms.

Table 2 Calculated structural parameters of $\alpha\text{-Ca}(\text{BH}_4)_2$.

Space Group	Fddd (No.70)		
Lattice constant (Å)	a = 8.802	b = 13.244	c = 7.473
Atom	x	y	z
Ca	0	0	0
B	0	0.2197	0
H1	-0.1133	0.2734	0.0132
H2	0.0020	0.1661	0.1360

Figure 3 depicts the total and partial densities of states for $\alpha\text{-Ca}(\text{BH}_4)_2$. The electronic structure is nonmetallic with a calculated gap of 4.9 eV. The valence states split into two peaks whose positions and widths are quite similar to those of LiBH_4 .⁽¹⁷⁾ The valence states are mainly composed of B and H orbitals and the contribution of Ca orbitals is hardly seen. This suggests an ionic character for the bonding between Ca and BH_4 . The Born effective charge tensor for Ca becomes diagonal due to the site symmetry and their values are predicted to be 2.08-2.43,⁽²³⁾ which are close to a nominal value of +2. This also supports an ionic picture for Ca.

Figure 4 depicts the phonon density of states calculated from the Γ -phonon frequencies as well as the result of Raman spectroscopy measurement. The

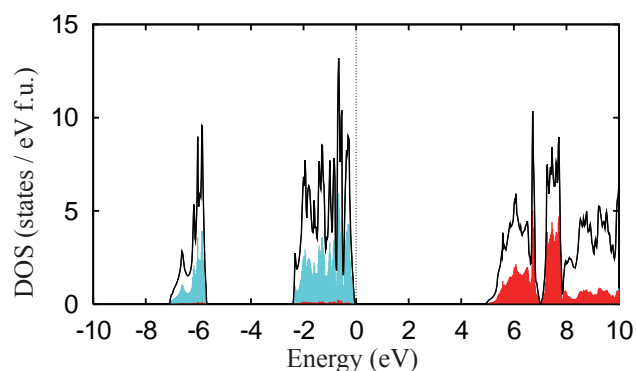


Fig. 3 Total and partial densities of states (DOS) for $\alpha\text{-Ca}(\text{BH}_4)_2$. The shaded-blue parts indicate the partial DOS for B and H atoms, and the red parts for the Ca atoms. The origin of energy is set to be the top of valence states.

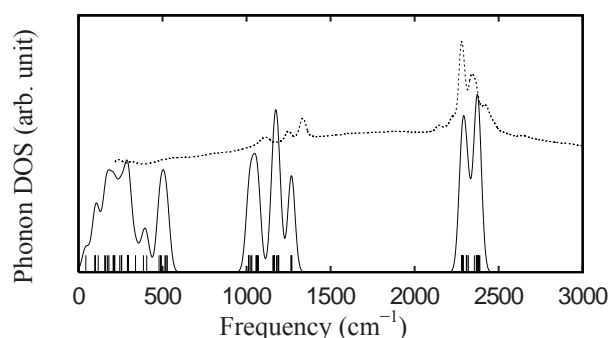
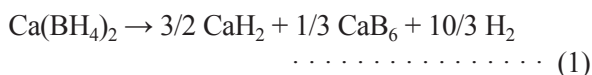


Fig. 4 Phonon density of states of $\alpha\text{-Ca}(\text{BH}_4)_2$. The contribution of the Γ -phonon modes indicated by vertical bars is only taken into account and the Gaussian broadening with of 30 cm^{-1} is used. The result of Raman spectroscopy measurement is also shown by a dotted line for comparison purposes.

Γ -phonon frequencies are classified into three groups. Analyzing the eigenvectors, we confirm that eigenmodes in the regions $1000\text{-}1300\text{ cm}^{-1}$ and $2250\text{-}2400\text{ cm}^{-1}$ originate from internal B-H bending and stretching vibrations of BH_4 complexes, respectively. These frequencies are in good agreement with the Raman experiment.⁽²³⁾ The eigenmodes with low frequencies ($<550\text{ cm}^{-1}$) include librational ones which involve the displacements of both Ca and BH_4 .

The thermodynamical stability is one of the most important properties for hydrogen storage materials, on which dehydrogenation temperature depends strongly. The dehydrogenating reaction for $\text{Ca}(\text{BH}_4)_2$ will be accompanied with the formation of CaH_2 and/or CaB_6 . The cohesive energies and the zero-point energies for $\alpha\text{-Ca}(\text{BH}_4)_2$ and related materials are listed in **Table 3**. Considering possible combinations of the products, the dehydrogenating reaction for $\alpha\text{-Ca}(\text{BH}_4)_2$ is expected to be



with the enthalpy change $\Delta H = 32\text{ kJ/mol H}_2$. The theoretical gravimetric density of the effective hydrogen is 9.6 mass%. The predicted ΔH is within the suitable range for hydrogen release under ambient conditions. In a thermodynamical view point, $\text{Ca}(\text{BH}_4)_2$ is thought to be a potential candidate for hydrogen storage materials.

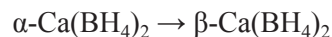
3.3 Crystal Structure of $\beta\text{-Ca}(\text{BH}_4)_2$

The Rietveld analysis pattern of the sample at temperature 433 K is shown in **Fig. 5**. This data are comprised of three phases and the phase ratio is 94.2,

Table 3 Calculated cohesive energies E_{coh} (eV/atom) and zero-point energies E_{zero} (meV/atom) for $\alpha\text{-Ca}(\text{BH}_4)_2$ and related materials. Note that the zero-point energies are not included in E_{coh} .

	E_{coh}	E_{ZPE}
$\text{Ca}(\text{BH}_4)_2$	3.302	192
Ca	1.845	20
B	6.201	126
H_2	2.272	135
CaH_2	2.694	117
CaB_6	5.987	109

4.5 and 1.3 mass% for $\beta\text{-Ca}(\text{BH}_4)_2$, $\gamma\text{-Ca}(\text{BH}_4)_2$ and $\alpha\text{-Ca}(\text{BH}_4)_2$, respectively. The $\alpha\text{-Ca}(\text{BH}_4)_2$ transforms to $\beta\text{-Ca}(\text{BH}_4)_2$ at approximately 433 K. It is expected that $\text{Ca}(\text{BH}_4)_2 \cdot \text{H}_2\text{O}$ is decomposed and transforms to $\gamma\text{-Ca}(\text{BH}_4)_2$.



By analyzing as $\text{P4}_2/\text{m}$ among possible space groups from the measured diffraction data, the most suitable values are obtained concerning the reliability factor R_{wp} , interatomic distances B-H and hydrogen thermal parameters B_{H} . This result agrees with the structure of $\beta\text{-Ca}(\text{BH}_4)_2$ and the theoretical investigation.^(27,40) However, the $\{100\}$ diffraction intensity, which should be appeared as $\text{P4}_2/\text{m}$, is not observed. It is expected that the arrangement of tetrahedron BH_4 or hydrogen atom positions are thermally disordered at high temperature.

In α - and $\beta\text{-Ca}(\text{BH}_4)_2$ structures, a boron atom bonds with four hydrogen atoms and forms a BH_4 tetrahedron. The arrangement of BH_4 tetrahedrons within (110) plane of $\alpha\text{-Ca}(\text{BH}_4)_2$ and the stacking of the planes are illustrated in **Fig. 2**. Similarly, (101) plane of $\beta\text{-Ca}(\text{BH}_4)_2$ is illustrated in **Fig. 6**. The layer of cation Ca^{2+} and anion BH_4^- are alternately stacking. Each phase of $\text{Ca}(\text{BH}_4)_2$ is the ionic crystals, and these layers are bound by electrostatic force.

In α - and $\beta\text{-Ca}(\text{BH}_4)_2$ structures, six boron atoms around a calcium atom coordinate in octahedral type. The arrangement of these octahedrons is illustrated in **Fig. 7**. Furthermore, three calcium atoms around a boron atom coordinate in plane triangle type in α - and

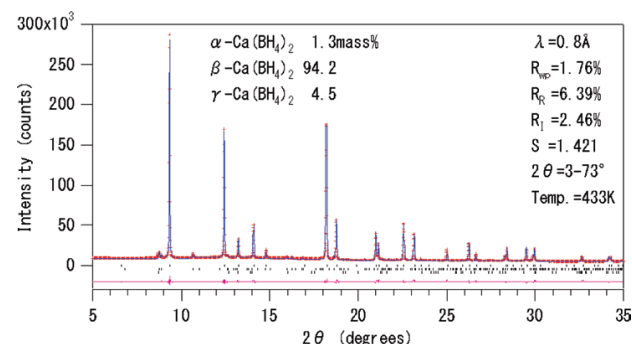


Fig. 5 Rietveld analysis pattern of the $\text{Ca}(\text{BH}_4)_2$ sample at 433 K.

β - $\text{Ca}(\text{BH}_4)_2$ structures. The α - $\text{Ca}(\text{BH}_4)_2$ structure connecting with the CaB_6 octahedrons which share four edges with the neighboring octahedrons. Two edges in β - $\text{Ca}(\text{BH}_4)_2$ are sharing with neighboring the CaB_6 octahedron. The polymorphism of $\text{Ca}(\text{BH}_4)_2$ is formed by connection sharing vertexes and edges of the CaB_6 octahedrons.

The 12 hydrogen atoms coordinate to a calcium atom in α - $\text{Ca}(\text{BH}_4)_2$ structure, because two hydrogen atoms within a BH_4 tetrahedron are located in the direction of a calcium atom. The range of distances between Ca and H are 2.24-2.61 Å in α - $\text{Ca}(\text{BH}_4)_2$. In β - $\text{Ca}(\text{BH}_4)_2$ structure, six BH_4 tetrahedrons around a calcium atom

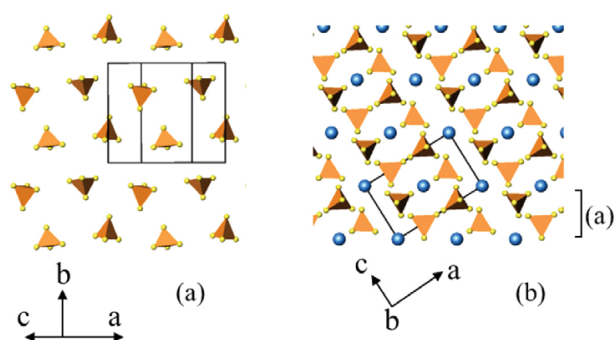


Fig. 6 (a) The arrangement of BH_4 tetrahedrons within the parallel plane to (101) plane, (b) the stacking of planes in β - $\text{Ca}(\text{BH}_4)_2$.

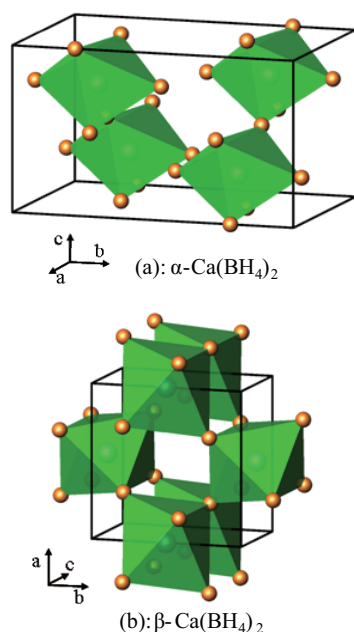


Fig. 7 The arrangement of CaB_6 octahedrons. The orange spheres represent B atoms.

are classified into two classes based on the Ca-H distance. Namely, the Ca-H distances are 2.52 and 2.54 Å in four BH_4 tetrahedrons and are 2.13, 3.02 and 3.02 Å in two BH_4 tetrahedrons.

3. 4 Dehydrating Properties of β - $\text{Ca}(\text{BH}_4)_2$

Figure 8 indicates TG, DTA, and MS profiles of the β - $\text{Ca}(\text{BH}_4)_2$ sample during heating process up to 800 K. The total weight loss evaluated by TG is 9.4 mass%, which is reasonably in agreement with the amount of hydrogen desorbed according to Eq. 1 (9.6 mass%). Endothermic peaks are observed at around 640 K and 720 K in the DTA profile and the weight losses appear in the corresponding temperature ranges of the TG profile. Furthermore, the sharp and broad dehydrogenation peaks are observed at the corresponding temperature ranges of the MS profile and no other impurity gases are detected within the accuracies of the MS apparatus. These results suggest the existence of an unknown intermediate compound for the reaction of Eq. 1 and two-step dehydrating reaction of the β - $\text{Ca}(\text{BH}_4)_2$. On the other hand, an endothermic peak at around 440 K reported by Kim et al.⁽⁴¹⁾ is not observed in our DTA profile. The endothermic peak observed in Ref. (41) is most likely

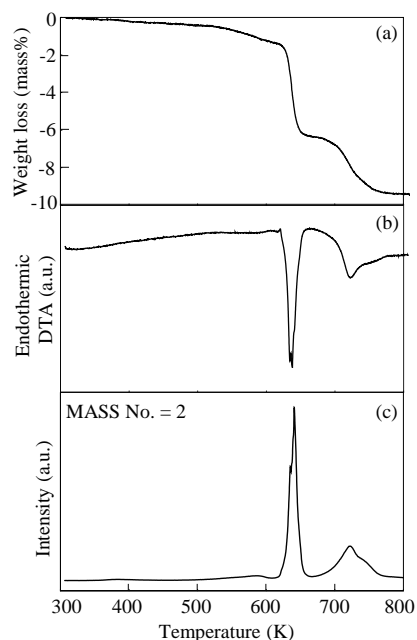


Fig. 8 (a) Thermogravimetry (TG), (b) differential thermal analysis (DTA), and (c) mass spectroscopy (MS) profiles during heating process of the β - $\text{Ca}(\text{BH}_4)_2$ sample. In the MS profile, other impurity gases are not detected within the accuracies of the apparatus.

originated from a structural phase transformation from α -Ca(BH₄)₂ into β -Ca(BH₄)₂.

In order to investigate its dehydriding reaction under hydrogen pressure, the *p-c* isotherm measurement for the β -Ca(BH₄)₂ is performed at 593 K (Fig. 9). The isotherm shows a plateau region at around 0.6 MPa, although this plateau pressure may be kinetically determined by the very slow reaction rate on Ca(BH₄)₂. The amount of the desorbed hydrogen during the *p-c* isotherm measurement was 5.9 mass%, which reasonably agrees with the amount of hydrogen desorbed up to 650 K in the TG profile (Fig. 8(a)). Therefore, the dehydriding reaction during the *p-c* isotherm measurement at 593 K is probably similar to that shown by the first endothermic peak in the DTA profile (Fig. 8(b)).

Figure 10 indicates the powder XRD profiles of the β -Ca(BH₄)₂ sample before and after the *p-c* isotherm measurement. The diffraction peaks of the β -Ca(BH₄)₂ phase are observed in the profile before the *p-c* isotherm measurement, which implies that the β -Ca(BH₄)₂ sample does not desorb hydrogen at 593 K under a hydrogen pressure of around 9.5 MPa. On the other hand, the CaH₂ phase and the intermediate phase can be seen in the profile after the *p-c* isotherm measurement. This result supports that the dehydriding reaction during the *p-c* isotherm measurement is similar to that at around 640 K under helium gas flow (Fig. 8), because the formation of the CaH₂ phase and the intermediate phase by heating up to 663 K has been

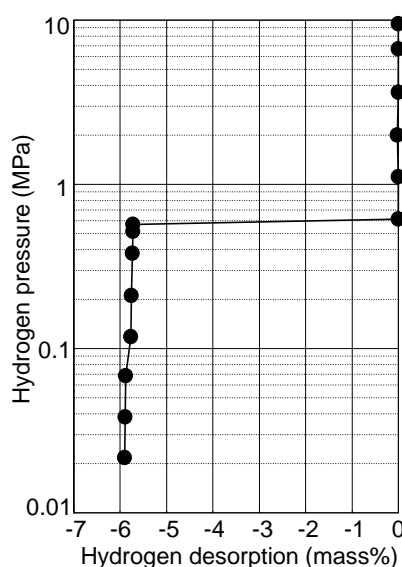


Fig. 9 A pressure-composition (*p-c*) isotherm of the β -Ca(BH₄)₂ in dehydriding process at 593 K.

reported.⁽⁴¹⁾ In order to investigate the crystal structure of the intermediate phase, we have conducted a synchrotron radiation XRD measurement. The inset in Fig. 10 shows the XRD profile measured at room temperature after the *p-c* isotherm measurement. By the analysis of this XRD profile using the Rietveld method, the intermediate phase was indexed on an orthorhombic lattice with the parameters $a = 4.0082(3)$ Å, $b = 3.8974(2)$ Å, and $c = 12.812(1)$ Å. More detailed investigations on the crystal structure of the intermediate phase are required to determine the dehydriding reaction pathways of Ca(BH₄)₂.

4. Conclusions

The polymorphic crystal structures of Ca(BH₄)₂ were investigated by the synchrotron powder X-ray diffraction measurement at SPring-8. The crystal structures of α -Ca(BH₄)₂ and β -Ca(BH₄)₂ were refined at temperature 300 and 433 K, respectively. The polymorphism of Ca(BH₄)₂ is formed by the different connection with adjacent octahedrons sharing vertexes

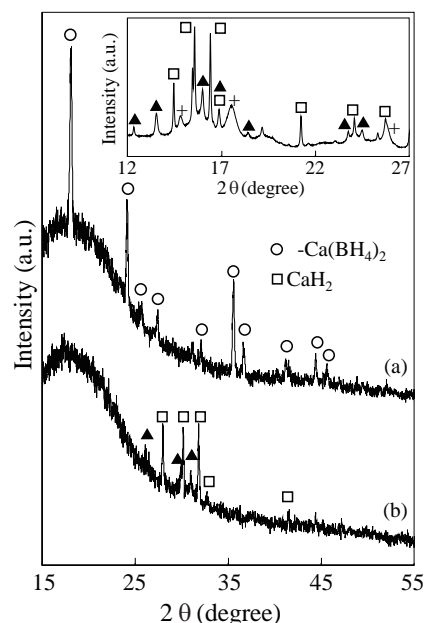


Fig. 10 Powder X-ray diffraction profiles of the β -Ca(BH₄)₂ (a) before and (b) after the *p-c* isotherm measurement at 593 K. The synchrotron radiation XRD profile of the sample after the *p-c* isotherm measurement is shown in the inset. Closed triangles show the peak positions of the orthorhombic intermediate phase. The diffraction peaks marked with crosses correspond to the Ca(OH)₂ phase formed by the reaction of the sample with moisture during the XRD measurement.

and edges of the CaB_6 octahedron. Using the structural information, the first-principles calculations have been performed to investigate the fundamental properties of $\text{Ca}(\text{BH}_4)_2$. The dehydriding reaction is predicted to be $\text{Ca}(\text{BH}_4)_2 \rightarrow 2/3\text{CaH}_2 + 1/3\text{CaB}_6 + 10/3\text{H}_2$, which is supported by the thermogravimetric analysis and the p - c isotherm measurement. The CaH_2 phase and the orthorhombic intermediate phase appeared in the XRD profile of the sample after the p - c isotherm measurement.

Acknowledgements

The authors would like to thank Dr. Y. Nakamori and Mr. K. Kikuchi for valuable discussion. The synchrotron radiation XRD measurements were performed in SPring-8 with the approval of the Japan Synchrotron Radiation Research Institute (JASRI) (Proposal No. 2006B0127 and No. 2007A1454). This work was partially supported by the New Energy and Industrial Technology Development Organization (NEDO), "Development of Safe Utilization Technology and an Infrastructure for Hydrogen Use (2005-2006)".

References

- (1) Crabtree, G. W., Dresselhaus, M. S., *MRS Bulletin*, Vol. 33, No. 4 (2008), pp. 421-428.
- (2) Schlapbach, L. and Züttel, A., *Nature*, Vol. 414 (2001), pp. 353-358.
- (3) Orimo, S., Nakamori, Y., Eliseo, J. R., Züttel, A. and Jensen, C. M., *Chem. Rev.*, Vol. 107 (2007), pp. 4111-4132.
- (4) Bogdanović, B. and Schwickardi, M., *J. Alloys Compd.*, Vol. 253-254 (1997), pp. 1-9.
- (5) Zidan, R. A., Takara, S., Hee, A. G. and Jensen, C. M., *J. Alloys Compd.*, Vol. 285 (1999), pp. 119-122.
- (6) Zaluski, L., Zaluska, A. and Ström-Olsen, J. O., *J. Alloys Compd.*, Vol. 290 (1999), pp. 71-78.
- (7) Gross, K. J., Guthrie, S., Takara, S. and Thomas, G., *J. Alloys Compd.*, Vol. 297 (2000), pp. 270-281.
- (8) Chen, P., Xiong, Z., Luo, J., Lin, J. and Tan, L., *Nature*, Vol. 420 (2002), pp. 302-304.
- (9) Orimo, S., Nakamori, Y., Kitahara, G., Miwa, K., Ohba, N., Noritake, T. and Towata, S., *Appl. Phys. A: Mater. Sci. Process.*, Vol. 79 (2004), pp. 1765-1767.
- (10) Luo, W., *J. Alloys Compd.*, Vol. 381 (2004), pp. 284-287.
- (11) Leng, H. Y., Ichikawa, T., Hino, S., Hanada, N., Isobe, S. and Fujii, H., *J. Phys. Chem. B*, Vol. 108 (2004), pp. 8763-8765.
- (12) Nakamori, Y., Kitahara, G., Miwa, K., Towata, S. and Orimo, S., *Appl. Phys. A: Mater. Sci. Process.*, Vol. 80 (2005), pp. 1-3.
- (13) Züttel, A., Wenger, P., Rentsch, S., Sudan, P., Mauron, Ph. and Emmenegger, Ch., *J. Power Sources*, Vol. 118 (2003), pp. 1-7.
- (14) Kojima, Y. and Hoga, T., *Int. J. Hydrogen Energy*, Vol. 28 (2003), p. 989.
- (15) Renaudin, G., Gomes, S., Hagemann, H., Keller, L. and Yvon, K., *J. Alloys Compd.*, Vol. 375 (2004), pp. 98-106.
- (16) Orimo, S., Nakamori, Y., Kitahara, G., Miwa, K., Ohba, N., Towata, S. and Züttel, A., *J. Alloys Compd.*, Vol. 404-406 (2005), pp. 427-430.
- (17) Miwa, K., Ohba, N., Towata, S., Nakamori, Y. and Orimo, S., *Phys. Rev. B*, Vol. 69 (2004), 245120.
- (18) Nakamori, Y., Miwa, K., Ninomiya, A., Li, H., Ohba, N., Towata, S., Züttel, A. and Orimo, S., *Phys. Rev. B*, Vol. 74 (2006), 045126.
- (19) Ohba, N., Miwa, K., Aoki, M., Noritake, T., Towata, S., Nakamori, Y., Orimo, S. and Züttel, A., *Phys. Rev. B*, Vol. 74 (2006), 075110.
- (20) Orimo, S., Nakamori, Y., Ohba, N., Miwa, K., Aoki, M., Towata, S. and Züttel, A., *Appl. Phys. Lett.*, Vol. 89 (2006), 021920.
- (21) Sullivan, E. A. and Wade, R. C., *Gravity Concentration to Hydrogen Energy, Kirk-Othmer Encyclopedia of Chem. Tech. Vol. 12, 3rd ed.*, (1980), p. 772, Wiley-Interscience.
- (22) Mackay, K. M., *Hydrogen Compounds of the Metallic Elements*, (1966), pp. 175-176, E. & F.N. SPON LTD.
- (23) Miwa, K., Aoki, M., Noritake, T., Ohba, N., Nakamori, Y., Towata, S., Züttel, A. and Orimo, S., *Phys. Rev. B*, Vol. 74 (2006), 155122.
- (24) Aoki, M., Miwa, K., Noritake, T., Ohba, N., Matsumoto, M., Li, H.-W., Nakamori, Y., Towata, S. and Orimo, S., *Appl. Phys. A*, Vol. 92 (2008), pp. 601-605.
- (25) Noritake, T., Aoki, M., Matsumoto, M., Miwa, K., Towata, S., Li, H.-W. and Orimo, S., *J. Alloy Compd.*, Vol. 491 (2010), pp. 57-62.
- (26) Rönnebro, E., E., Majzoub, H., *J. Phys. Chem. B*, Vol. 111 (2007), pp. 12045-12047.
- (27) Lee, Y.-S., Kim, Y., Cho, Y. W., Shapiro, D., Wolverton, C. and Ozolins, V., *Phys. Rev. B*, Vol. 79 (2009), 104107.
- (28) Aoki, M., Noritake, T., Kitahara, G., Nakamori, Y., Towata, S. and Orimo, S., *J. Alloys Compd.*, Vol. 428 (2007), pp. 307-311.
- (29) Nakamori, Y., Kitahara, G., Ninomiya, A., Aoki, M., Noritake, T., Towata, S. and Orimo, S., *Mater. Trans.*, Vol. 46 (2005), pp. 2093-2097.
- (30) Nakamori, Y., Ninomiya, A., Kitahara, G., Aoki, M., Noritake, T., Miwa, K., Kojima, Y. and Orimo, S., *J. Power Sources*, Vol. 155 (2006), pp. 447-455.
- (31) Nishibori, E., Takata, M., Kato, K., Sakata, M., Kubota, Y., Aoyagi, S., Kuroiwa, Y., Yamakata, M. and Ikeda, N., *Nucl. Instr. and Meth. A*, Vol. 467-468 (2001), pp. 1045-1048.
- (32) Izumi, F. and Ikeda, T., *Mater. Sci. Forum*, Vol. 321-324 (2000), p. 198.
- (33) Vanderbilt, D., *Phys. Rev. B*, Vol. 41, No. 11 (1990), pp. 7892-7895.

- (34) Hohenberg, P. and Kohn, W., *Phys. Rev.*, Vol. 136, No. 3B (1964), pp. B864-B871.
- (35) Kohn, W. and Sham, L. J., *Phys. Rev.*, Vol. 140, No. 4A (1965), pp. A1133-A1138.
- (36) Perdew, J. P., Burke, K. and Ernzerhof, M., *Phys. Rev. Lett.*, Vol. 77, No. 18 (1996), pp. 3865-3868.
- (37) Ohba, N., Miwa, K., Nagasako, N. and Fukumoto, A., *Phys. Rev. B*, Vol. 63 (2001), 115207.
- (38) Gonze, X. and Lee, C., *Phys. Rev. B*, Vol. 55, No. 16 (1997), pp. 10355-10368.
- (39) Kunc, K. and Martin, R. M., *Phys. Rev. Lett.*, Vol. 48, No. 6 (1982), pp. 406-409.
- (40) Buchter, F., Łodziana, Z., Remhof, A., Friedrichs, O., Borgschulte, A., Mauron, Ph., Züttel, A., Sheptyakov, D., Barkhordarian, G., Bormann, R., Chłopek, K., Fichtner, M., Sørby, M., Riktor, M., Hauback, B. and Orimo, S., *J. Phys. Chem. B*, Vol. 112 (2008), pp. 8042-8048.
- (41) Kim, J., Jin, S., Shim, J. and Cho, Y.W., *J. Alloys Compd.*, Vol. 461 (2008), pp. L20-L22.

Figs. 1, 2, 5, 6 and Table 1

Reprinted from *J. Alloys Compd.*, Vol. 491 (2010), pp. 57-62, Noritake, T., Aoki, M., Matsumoto, M., Miwa, K., Towata, S., Li, H.-W. and Orimo, S., "Crystal Structure and Charge Density Analysis of $\text{Ca}(\text{BH}_4)_2$ ", © 2010 Elsevier, with permission from Elsevier.

Fig. 7

Text

- p.43 left 1.2 - 1.11
- p.44 left 1.19 - 1.38
- p.46 left 1.30 - right 1.7
- p.46 right 1.19 - p.47 right 1.4
- p.48 right 1.14 - 1.18

Adapted from *J. Alloys Compd.*, Vol. 491 (2010), pp. 57-62, Noritake, T., Aoki, M., Matsumoto, M., Miwa, K., Towata, S., Li, H.-W. and Orimo, S., "Crystal Structure and Charge Density Analysis of $\text{Ca}(\text{BH}_4)_2$ ", © 2010 Elsevier, with permission from Elsevier.

Figs. 3, 4, Tables 2 and 3

Reprinted from *Phys. Rev. B*, Vol 74 (2006), 155122, Miwa, K., Aoki, M., Noritake, T., Ohba, N., Nakamori, Y., Towata, S., Züttel, A. and Orimo, S., "Thermodynamical Stability of Calcium Borohydride $\text{Ca}(\text{BH}_4)_2$ ", © 2006 APS, with permission from American Physics Society.

Figs. 8-10

Text

- p.43 right 1.16 - p.44 left 1.7
- p.44 left 1.13 - 1.18
- p.48 left 1.9 - 1.12

Reprinted from *Appl. Phys. A*, Vol. 92 (2008), pp. 601-605, Aoki, M., Miwa, K., Noritake, T., Ohba, N., Matsumoto, M., Li, H.-W., Nakamori, Y., Towata, S. and Orimo, S., "Structural and Dehydrogenating Properties of $\text{Ca}(\text{BH}_4)_2$ ", © 2008 Springer, with permission from Springer.

Masakazu Aoki

Research Field:

- Material Science

Academic Degree: Ph.D

Academic Society:

- The Japan Institute of Metals and Materials



Kazutoshi Miwa

Research Fields:

- Computational Material Physics

- Hydrogen Storage Materials

Academic Degree: Dr.Eng.

Academic Societies:

- American Physical Society

- The Japan Institute of Metals and Materials

- The Physical Society of Japan

Award:

- American Physical Society, Outstanding Referee, 2013



Tatsuo Noritake

Research Field:

- Crystal Structure Analysis of Hydrogen Storage Materials

Academic Degree: Ph.D

Academic Societies:

- The Japan Institute of Metals and Materials

- The Chemical Society of Japan



Hai-Wen Li*

Research Fields:

- Hydrogen Storage

- Functional Materials

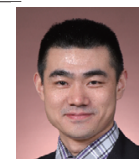
Academic Degree: Dr.Eng.

Academic Societies:

- The Japan Institute of Metals

- Hydrogen Energy Systems Society of Japan

- Materials Research Society



Shin-ichi Orimo**

Research Fields:

- Fundamental and Energy-related Application of Advanced Hydrides
- Materials Engineering and Materials Chemistry



Academic Degree: Ph.D

Academic Societies:

- The Japan Institute of Metals
- The Japan Society of Applied Physics
- Hydrogen Energy Systems Society of Japan

Awards:

- Best Scientific Paper Award, The Japanese Institute of Metals, 1997
- Best Young Researcher Award, The Japanese Institute of Metals, 1998
- Research Award, Materials Science Foundation, 2002
- Promoted Research Award, Japan Magnesium Association, 2003
- Intelligent Cosmos Prize, Intelligent Cosmos Foundation, 2004
- Murakami Memorial Encouraged Research Award, 2004
- Technical Development Award, The Japanese Institute of Metals, 2008
- Best Scientific Paper Award, Japan Copper and Brass Association, 2011
- Funding Program for Next Generation World-leading Researchers Cabinet Office, Council for Science and Technology Policy, JSPS, 2011
- Metals Meritorious Award, The Japanese Institute of Metals, 2011
- Prize for Science and Technology, Research Category, The Commendation for Science and Technology by the Minister, MEXT, 2012

* Kyushu University

** Tohoku University